The effects of initial perturbation to mixing-layer noise

Lin Zhou,[1] Zhenhua Wan,[1] Dejun Sun,[1, a)] and Mingjun Wei[2, b)]

[1)] *Department of Modern Mechanics, University of Science and Technology of China, Hefei 230022, China*

[2)] *Department of Mechanical and Aerospace Engineering, Las Cruces, New Mexico State University, USA.*

(Received 10 March 2011; accepted 10 April 2011; published online 10 May 2012)

Abstract The far-field noise radiated from mixing layers is determined by the near-field flow dynamics which is sensitive to the initial perturbation of instability introduced physically or numerically. This study focuses on the effects of the phase delay in two initial perturbations, one at the fundamental wave number and the other at its subharmonic both calculated from linear instability analysis, on the sound generation in mixing layers. When different phase delays ϕ_1 changing from zero to 2π is applied on the fundamental mode, we observe different vortex merging processes (e.g. vortex pairing or tearing). The strong nonlinear interaction in the merging process generates most of the noise from mixing layers. There shows a pattern in a period of 2π for the response of far-field sound to the change of ϕ_1. Similar effects on the dynamics and acoustics can be achieved by adding different phase delays ϕ_2 to the subharmonic mode instead, however, the response repeats in a period of only π for ϕ_2. The effects of the combination of different phase delays to other parameters, including the amplitude and wave number for each perturbations, are also investigated. All the results indicate a critical role of nonlinearity in the sound generation mechanism of mixing layers. [doi:10.1063/2.1203203]

Keywords nonlinear interaction, instability, mixing-layer noise

It has been a long journey for the study of noise generation from free shear layers since Lighthill's pioneer work.[1] There were many works on this topic through different approaches experimentally,[2] numerically,[3] and theoretically[4] in the past half century. It is commonly agreed that in subsonic free shear layers there are two types of sound sources,[5] namely large-scale coherent structures and turbulent fine structures, and the former one normally plays the dominant role. The development of large coherent structures (e.g. vortex roll-up, pairing, and tearing) can often be explained by the evolution of instability waves in the flow.[6,7] For supersonic flows, the sound radiation mechanism is related to the linear instability waves, which mostly travel at supersonic phase speed and therefore are radiation capable.[8] On the other hand, the noise radiation mechanism for subsonic flows is less obvious for the globally subsonic phase speed of their linear instability waves. So that, nonlinearity and the interaction between instability waves are critical in the noise radiation of subsonic shear flows.[9] A simple mixing layer, developing temporally or spatially, has three developing stages which can all be explained by the behaviors of instability waves: the first is the initial vortex roll-up which is the growth of the most unstable instability wave; the second is the vortex interaction such as pairing, tearing, and merging, which is from the competition and nonlinear interaction of instability waves at different frequencies and with different phase delays; last, when all instability waves go stable at larger shear-layer thickness, the near-field dynamics is dominantly viscous damping. Among these stages, most noise is generated in the second stage with strong nonlinear interaction. There is also clear indication of the sensitivity of the nonlinear interaction to the initial perturbations implemented to introduce instability.[10] Therefore, the current study focuses on the understanding of the correlation between the phase delay in initial perturbations and sound generation in mixing layers. In this work, we choose a temporally-developing mixing layer for its simplicity and the capability of resembling a spatially-developing mixing layer in key dynamics[11,12] and aeroacoustics.[13] The periodic boundary condition for temporal-developing flows also brings in computational convenience and clarity in the implementation of the initial perturbations for instability.

The basic computational setup is shown schematically in Fig. 1, where the Mach number of lower and upper flows are $M_1 = 0.25$ and $M_2 = 0.50$, respectively, and the Reynolds number based on far-field sound speed and initial vorticity thickness is $Re = \rho_\infty a_\infty \delta_\omega / \mu = 1\,000$. The initial flow profile is a boundary layer solution superposed by small perturbation with two normal modes,

$$q'(\phi_1, \phi_2; x, y) = C \sum_{k=1}^{2} \mathscr{R} \left\{ A_k \hat{q}_k(y) \mathrm{e}^{\mathrm{i}(\alpha_k x + \phi_k)} \right\}, \tag{1}$$

where $\mathscr{R}$ denotes the real part, C is an arbitrary small number to limit the overall perturbation strength, A_k defines the amplitude of individual instability waves, $\hat{q}_k(y)$ is the eigen-modes computed by linear instability theory, α_k is the wave number, and ϕ_k is the phase delay

a) Corresponding author. Email: dsun@ustc.edu.cn.

b) Email: mjwei@nmsu.edu.

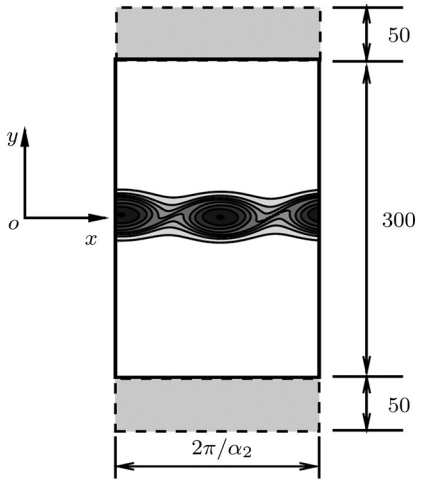

Fig. 1. The schematic for the computational configuration of the current temporally-developing mixing layer: gray areas at the top and bottom mark for computational sponge zones.

of each modes. In the current study, we only choose two wave numbers: the fundamental mode α_1 and its subharmonic $\alpha_2(=\alpha_1/2)$, which present the nonlinear interaction as resonance.[9] The instability modes $\hat{q}_k(y)$ are calculated from linear instability analysis using spectral collocation method and shown in Fig. 2. The amplitudes of the modes are normalized,[14] and the initial phases are adjusted to make the imaginary part of $\hat{v}$ equal to 0 at $y = 0$. So that, the current study of phase delay is independent of the phase difference caused by different computational approaches in solving instability modes.

The computational domain is $[0, 2\pi/\alpha_2]$ along x direction with periodic boundary condition and $[-200, 200]$ along y direction with sponge zones at both ends $[-200, -150]$ and $[150, 200]$, where the lengths are non-dimensionalized by initial vorticity thickness δ_ω. Spectral method is used to solve the derivatives along x, a fourth-order dispersion-relation-preserving scheme[15] is used to solve the derivatives along y for easy code parallelization, and a fourth-order Runge-Kutta scheme is used for time advancement. All the algorithm and code have been used and extensively validated in our previous works.[11,16–18]

To study the effects of initial phase delays, we pick six cases shown as case K_{1a} to case K_5 in Table 1, where K_{1a} and K_{1b} are considered the base cases focusing on the variations (as sub-cases) of ϕ_1 and ϕ_2 respectively from 0 to 2π, and K_2 to K_5 have the same range of in phase delays as in K_{1b} (on ϕ_2) but with difference in initial amplitudes and wave numbers to study the combined effects from these additional parameters. It is noted that the overall energy is kept low by using small amplitudes in all cases (except for K_2) to ensure the appearance of the nonlinear mechanism.[9]

For all the cases, the disturbance energy of individual instability waves is amplified linearly at first, then there is the strong nonlinear interaction between the

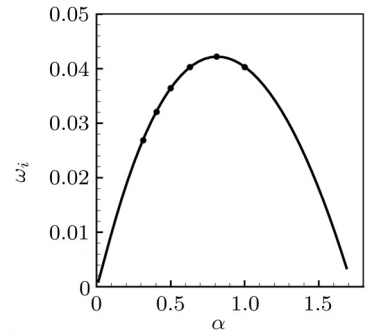

(a) Growth rate ω_i as a function of wave number α

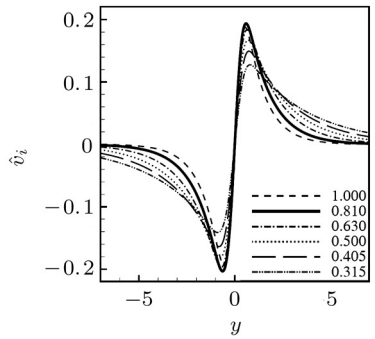

(b) Imaginary part of eigenfunction $\hat{v}$ for different wave numbers (marked in (a) by filled circles), where $\alpha = 0.810$ is the most unstable wave number and marked in thick solid line

Fig. 2. The results of linear instability analysis.

Table 1. Parameters for different numerical cases to study the effects of phase delays and other characteristics of initial perturbations in form of instability modes.

Case	C	A_1	A_2	α_1	α_2	ϕ_1	ϕ_2
K_{1a}	0.001	1.0	1.00	0.81	0.405	$0 \sim 2\pi$	0.0
K_{1b}	0.001	1.0	1.00	0.81	0.405	0.0	$0 \sim 2\pi$
K_2	0.001	1.0	10.0	0.81	0.405	0.0	$0 \sim 2\pi$
K_3	0.001	1.0	0.10	0.81	0.405	0.0	$0 \sim 2\pi$
K_4	0.001	1.0	1.0	0.63	0.315	0.0	$0 \sim 2\pi$
K_5	0.001	1.0	1.0	1.00	0.500	0.0	$0 \sim 2\pi$

fundamental mode and the subharmonic mode. Such strong interaction in near-field dynamics produces the majority of noise at the far field. Here, to indicate the energy level of far-field sound, we use density perturbation $\langle\rho'\rangle$ spatially-averaged along a line at $Y = -100$ and parallel to the streamwise,[19] though the averaged sound intensity should serve the same purpose well.

Figure 3(a) shows the evolution of $\langle\rho'\rangle$ in case K_{1a} at $Y = -100$ versus the delayed time $t_\mathrm{d} = t - |Y|/a_\infty$. Two critical moments A and B are marked in Fig. 3(a): A is the moment for the disturbance energy of α_1 to reach the maximum growth rate, and B is for the disturbance energy of subharmonic $\alpha_2 = \alpha_1/2$ to reach the maximum growth rate. Both are in the sense of the de-